Order Number 1349124

Analysis of unsteady flow through an earthen dam using the boundary element method

Shaheed, Salma, M.S.

The University of Arizona, 1992

U·M·I
300 N. Zeeb Rd.
Ann Arbor, MI 48106

ANALYSIS OF UNSTEADY FLOW THROUGH AN EARTHEN DAM USING THE BOUNDARY ELEMENT METHOD

by

Salma Shaheed

A Thesis Submitted to the Faculty of the

DEPARTMENT OF CIVIL ENGINEERING AND ENGINEERING MECHANICS

In Partial Fulfillment of the Requirements
For the Degree of

MASTER OF SCIENCE

WITH A MAJOR IN CIVIL ENGINEERING

In the Graduate College

THE UNIVERSITY OF ARIZONA

1 9 9 2

STATEMENT BY AUTHOR

This thesis has been submitted in partial fulfillment of requirements for an advanced degree at The University of Arizona and is deposited in the University Library to be made available to borrowers under the rules of the Library.

Brief quotations from this thesis are allowable without special permission, provided that accurate acknowledgement of source is made. Requests for permission for extended quotation from or reproduction of this manuscript in whole or in part may be granted by the head of the major department or the Dean of the Graduate College when in his or her judgement the proposed use of the material is in the interests of scholarship. In all other instances, however, permission must be obtained from the author.

Signed: Salman Shahid

APPROVAL BY THESIS DIRECTOR

This thesis has been approved on the date shown below:

Dinshaw N. Contractor

Dinshaw N. Contractor
Professor of Civil Engineering

6/23/92

Date

ACKNOWLEDGMENTS

With fondness and appreciation, I would like to express my sincere gratitude to my advisor, Professor Dinshaw N. Contractor, for his generous and valuable guidance, suggestions, encouragement and support during this research work. I would also like to thank Dr. Muniram Budhu and Dr. Panos D. Kiousis for being members of my master's committee and for reviewing this work and offering helpful suggestions.

I would like to extend my sincere thanks to my family and relatives in Bangladesh for all of their supports and encouragement during my graduate studies at The University of Arizona.

Finally, I am greatly indebted to my husband Zakaria and daughter Nazifa who were the main source of inspiration during this work.

TABLE OF CONTENTS

LIST OF ILLUSTRATIONS

ABSTRACT

Unsteady flow through an earthen dam has been investigated using the Boundary Element Method in which the upstream reservoir level may vary in a cyclic manner. The seepage surface at the upstream face is included in the computer model when the water level drops in the upstream reservoir. The use of this model has been illustrated by studying the variation of the phreatic surface in a beach along the Colorado river in the Grand Canyon. The potentials at various internal points are also calculated and compared with those measured in the field. Very good agreement is obtained between the results using the Boundary Element Method and field data.

CHAPTER 1

INTRODUCTION

Analysis of unsteady flow in an earthen dam including the pressure or potential variation within the dam is very important for the design of the earthen dam. Earthen dams are used to protect the land in the regions where the water levels may rise and fall in a cyclic manner [1]. Repeated rising and falling of upstream water level causes large variations of pressure and stress inside the dam. Since, soil is a non linear material, repeated variation of pressure or stress (from high pressure to low pressure) leads to an increase of total deformation within the soil mass after each cycle [2], which may ultimately cause the failure of the earthen dam. The principal causes of dam failure are surface erosion, piping and sliding within the dam or foundation.

Determination of pressure variation inside the earthen dam for unsteady flow can be performed physically, analytically and numerically. But the physical method is time consuming, expensive and laborious and sometimes it is not possible to obtain accurate data because of human error, weather condition etc. Exact analytical solutions for unsteady flow are difficult to obtain. So, with the availability of high speed computers, numerical solutions have been developed by using different numerical methods. In the early stage, the finite difference method was used extensively to solve problems dealing with flow through porous media. But

for unsteady flow, the use of finite difference method is not widely used because of its limitation to geometrical adjustment and to apply boundary conditions to the geometry and its complexity in dealing with nonhomogeneous and anisotropic media.

The finite element method was developed and is now replacing the finite difference method as the dominant technique. This method has several advantages, such as ease of conforming to the physical geometry and ease of applying boundary conditions. Variable grid spacing can be used and universal programs can be written to apply to any geometry and to a large number of physically different situations. But there are some disadvantages in the finite element method. The primary disadvantages are the time consuming data input of the grid and long computing time, especially for complex problems and three-dimensional problems because of large number of nodes. Lately the boundary element method has been developed as an alternative. The advantages of the boundary element method over finite element method are:

1. Boundary element method is a direct method because the governing differential equation or differential operator is solved exactly and all the approximation is confined to the boundary. This method is also known as inverse method because in this method the functions which are considered, identically satisfy the governing equations in the domain and approximately satisfy the boundary conditions. So, the main concern is to choose the boundary element such that the variables are approximated accurately on the boundary which can be made from one's physical knowledge of the problem. In contrast, in finite element method, the assumed functions satisfy the

boundary conditions and are approximated in the domain, i.e., not satisfying exactly the governing equation.

2. In case of unsteady flow, the following Laplace equation with appropriate boundary conditions is used in the boundary element method:

$$\nabla^2\phi = \frac{\partial^2\phi}{\partial x^2} + \frac{\partial^2\phi}{\partial y^2} + \frac{\partial^2\phi}{\partial z^2} = 0 \tag{1.1}$$

which is simple and independent of time and physical constants such as hydraulic conductivity and specific storage. In the finite element method, the following Poisson equation is used:

$$\nabla^2\phi = \frac{\partial^2\phi}{\partial x^2} + \frac{\partial^2\phi}{\partial y^2} + \frac{\partial^2\phi}{\partial z^2} = \frac{s_e}{k}\frac{\partial\phi}{\partial t} \tag{1.2}$$

which accounts for physical constants such as specific storage s_e, hydraulic conductivity, k and is time dependent. Thus the equation and the algorithm process in finite element method for unsteady flow through an earthen dam is more complicated than in the boundary element method.

3. The Boundary element method requires less time-consuming data input and shorter computing time than the finite element method, especially for complex and three-dimensional problems, because the boundary element method needs line integration for two-dimensional and surface integration for three-dimensional problems. In contrast, the finite element method requires volume discretization for three-dimensional and area discretization for two-dimensional problems.

4. In the case of flow through an earthen dam, by using the boundary element method, it is possible to apply the boundary conditions at the seepage face

directly to the boundary. In the finite element method approximations are used to handle the seepage surface e.g an arbitrary area is assumed such that the phreatic surface meets the reservoir directly [3,4] or impervious boundary condition (no flow through the seepage surface) is assumed [5,6].

It is clear from the above discussion, that a very good solution can be obtained for unsteady flow through an earthen dam using the boundary element method. The analysis of steady and unsteady flow through an earthen dam has been studied by Liggett [7,8] using boundary element method. In his study, for unsteady flow the first model is investigated assuming sudden drawdown from a high water level to a lower water level at the downstream face. In his second model it is considered that the water level on the upstream face can rise with time, but the water level cannot decrease since there is no provision for seepage surface on the upstream face.

In this study, considering the real situation in the field where water level on the upstream face can rise and fall, unsteady flow through an earthen dam has been analyzed including the seepage surface on the upstream side. Thus, the objectives of this study are:

1. To develop a computer model for unsteady flow through an earthen dam by using boundary element method which accounts for rising and falling of the water level on the upstream face.

2. To apply this model to a field situation and compare the results of this model with the measured data.

CHAPTER 2

BOUNDARY ELEMENT METHOD

2.1 General

The boundary element method is one of several numerical methods of analysis for the solution of flow through porous media, whose governing equation is the classical Laplace equation. This method uses integral equations that are obtained from the transformation of the basic partial differential equation describing the behavior of the unknown variable on the boundary. Thus in this method, only the boundary needs to be discretized. The variables at internal points are then calculated from the boundary solution. Since all numerical approximations take place at the boundaries, the dimensionality of the problem (line integration for two-dimensional and surface integration for three-dimensional problem) is reduced by one and a smaller system of equations is obtained in comparison with those determined through other methods e.g finite element method, with sufficient accuracy. The integral equation represents a relationship between the unknown (potential for fluid flow) and the source density or free space Green's function. The Green function is the potential for three-dimensional problems or the logarithmic potential for two-dimensional problems and is called the fundamental solution to Laplace's equation. To find the unknowns on the boundary, the boundary is discretized into a series of small segments. The discretized equation is applied successively to all the nodes in the network, and the influence coefficients are computed. This results

in a system of linear algebraic equations which can be readily solved. The governing boundary integral equations for two-dimensional free surface flow problems are presented in the following section.

2.2 Integral Equations for 2-D flow problem

The expression of continuity in a two-dimensional plane can be written in terms of the divergence theorem as:

$$\int_D (\nabla \cdot v) dA = \int_\Omega v \cdot n dS \tag{2.1}$$

Where ∇ is the vector operator, v is any differentiable vector, D is the domain of integration, Ω is the boundary of D and n is the unit outward normal to D on Ω.

If we take v as $U\nabla W$ or $W\nabla U$, where U and W are two functions, twice differentiable in D, such that the Equation 2.1 can be written as

$$\int_D \left(U\nabla^2 W - W\nabla^2 U \right) dA = \int_\Omega \left(U\nabla W - W\nabla U \right) \cdot n dS \tag{2.2}$$

The above equation is *Green's* second identity. Substituting $\nabla W \cdot n = \frac{\partial W}{\partial n}$ and $\nabla U \cdot n = \frac{\partial U}{\partial n}$, the above equation follows

$$\int_D \left(U\nabla^2 W - W\nabla^2 U \right) dA = \int_\Omega \left(U\frac{\partial w}{\partial n} - W\frac{\partial U}{\partial n} \right) dS \tag{2.3}$$

In Equation 2.3, U & W are chosen such that they satisfy Laplace's equation, i.e., $\nabla^2 U = \nabla^2 W = 0$. Then the Equation 2.3 becomes as [8]

$$\int_\Omega \left(U\frac{\partial W}{\partial n} - W\frac{\partial U}{\partial n} \right) dS = 0 \tag{2.4}$$

In the case of the potential problem, U is chosen as a velocity potential, ϕ, and W is chosen as a 'free space Green's function' which satisfies $\nabla^2 W = 0$ everywhere in D except at the source point P as shown in Figure 2.1 where it becomes infinity. For two-dimensional problems, the free space green function, W is chosen [9] as

$$W = ln(r) \tag{2.5}$$

in which r is the distance between the source point P inside the boundary and the field point Q on the boundary as shown in Figure 2.1. In order to apply Equation 2.4 to find the potential at P, the point P is excluded by a small circle of radius r_o to avoid the singularity. Thus the integral Equation 2.4 follows as

$$\int_\Gamma \left(\phi \frac{\partial ln(r)}{\partial n} - ln(r)\frac{\partial \phi}{\partial n}\right) dS + lim_{r_o \to 0} \int_\sigma \left(\phi \frac{\partial ln(r_o)}{\partial n} - ln(r_o)\frac{\partial \phi}{\partial n}\right) dS = 0 \tag{2.6}$$

Upon applying the limit to the second integral of Equation 2.6, it follows

$$lim_{r_o \to 0} \int_\sigma \left(- \phi \frac{\partial ln(r_o)}{\partial n} - ln(r_o)\frac{\partial \phi}{\partial r}\right) r_o d\theta = -2\pi\phi(P) \tag{2.7}$$

Since,

$$lim_{r_o \to 0} ln(r_o) r_o = 0 \tag{2.8a}$$

and

$$\frac{\partial ln(r)}{\partial n} = \frac{1}{r}\frac{\partial r}{\partial n} = \frac{1}{r}(\nabla r \cdot n) = -\frac{1}{r} \tag{2.8b}$$

around the circle σ.

Equation 2.6 can be written as

$$2\pi\phi(P) = \int_\Gamma \left(\phi(Q)\frac{\partial ln(r)}{\partial n} - ln(r)\frac{\partial \phi(Q)}{\partial n}\right) dS \tag{2.9}$$

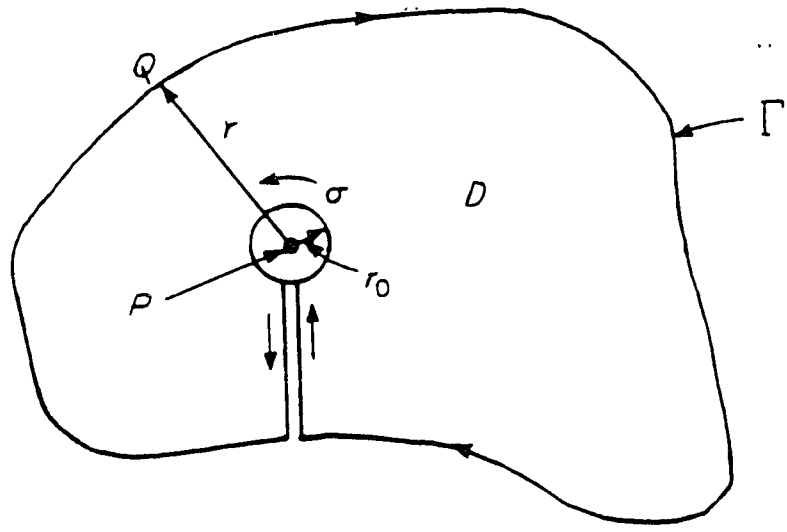

Figure 2.1. Domain D surrounded by the boundary curve Γ and the singular point P is separated from D by the circle σ

To find the potential inside the boundary, ϕ and $\frac{\partial \phi}{\partial n}$ must be known everywhere on the boundary. Since, both ϕ and $\frac{\partial \phi}{\partial n}$ are not all known, the point P is moved to the boundary to complete the boundary data as shown in Figure 2.2. The same consideration holds as before except that the integration as indicated in Equation 2.9 takes place over an angle which is less than 2π. Therefore, the Equation 2.9 is need to be modified as

$$c\phi(P) = \int_{\Gamma} \left(\frac{\phi}{r} \frac{\partial r}{\partial n} - ln(r) \frac{\partial \phi}{\partial n} \right) dS \tag{2.10}$$

In which c is the angle between the boundary segment at P as shown in Figure 2.2 and is equal to 2π for an internal point. As shown in Figure 2.3, the boundary data is completed by discretizing the boundary and considering the representative source point as (i) and field points as (j, j+1).

If N is the total number of elements and nodes for a closed boundary, for each source point i, an equation which relates ϕ and $\frac{\partial \phi}{\partial n}$ over all elements is obtained. In that case from Equation 2.10 it can be written as

$$c\phi(i) = \int_{\Gamma} \left(\frac{\phi}{r} \frac{\partial r}{\partial n} - ln(r) \frac{\partial \phi}{\partial n} \right) d\Gamma = \sum_{j=1}^{N} \int_{\alpha_{ij}}^{\alpha_{ij}+l_j} \left(\frac{\phi}{r} \frac{\partial r}{\partial n} - ln(r) \frac{\partial \phi}{\partial n} \right) d\alpha \tag{2.11}$$

Assuming a linear variation of potential and its normal derivatives between the nodes in the element such that

$$\phi = \frac{\alpha_{ij} + l_j - \alpha}{l_j} \phi_j + \frac{\alpha - \alpha_{ij}}{l_j} \phi_{j+1} \tag{2.12a}$$

$$\frac{\partial \phi}{\partial n} = \frac{\alpha_{ij} + l_j - \alpha}{l_j} \left(\frac{\partial \phi}{\partial n} \right)_j + \frac{\alpha - \alpha_{ij}}{l_j} \left(\frac{\partial \phi}{\partial n} \right)_{j+1} \tag{2.12b}$$

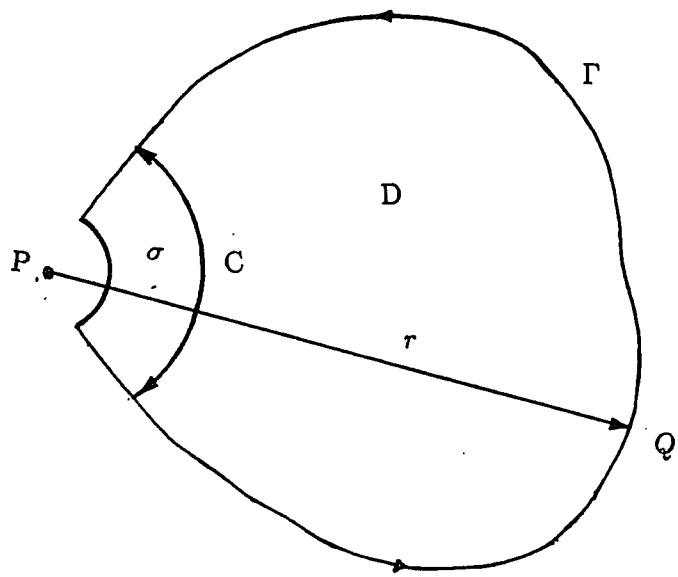

Figure 2.2. Point P on the boundary where the boundary contour forms an angle

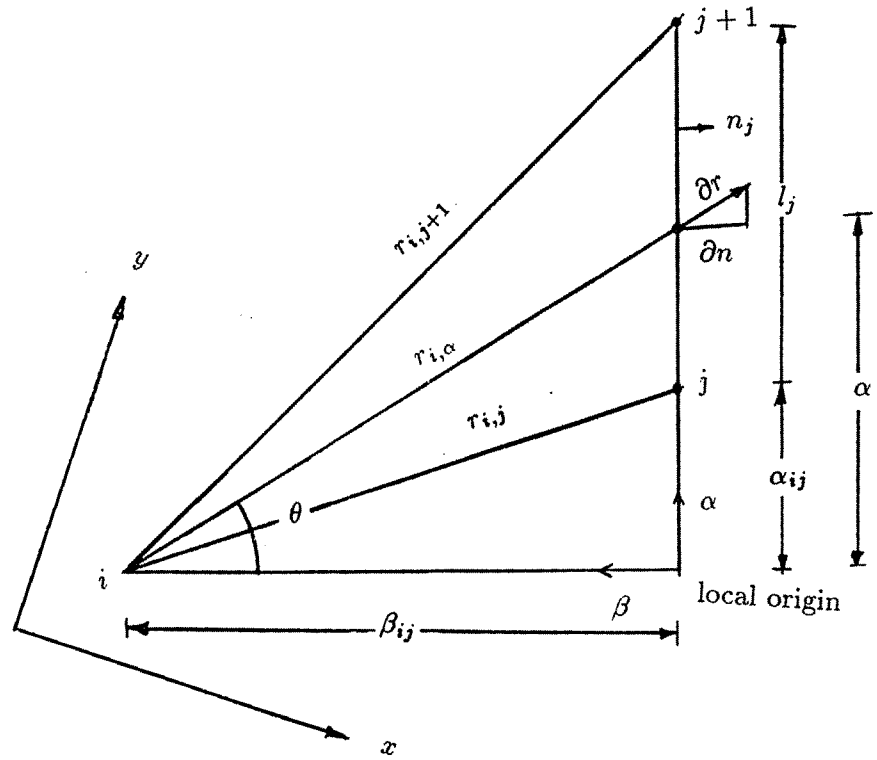

Figure 2.3. $\alpha - \beta$ coordinate system (Non singular case)

and from Figure 2.3

$$\frac{\partial r}{\partial n} = cos\theta = \frac{\beta_{ij}}{r_{i,\alpha}} \tag{2.12c}$$

Then the Equation 2.11 becomes

$$\int_{\alpha_{ij}}^{\alpha_{ij}+l_j} \left(\frac{\phi}{r}\frac{\partial r}{\partial n} - ln(r)\frac{\partial \phi}{\partial n}\right) d\alpha = \int_{\alpha_{ij}}^{\alpha_{ij}+l_j} \frac{\beta_{ij}}{r_{i\alpha}^2}\left[\frac{\alpha_{ij}+l_j-\alpha}{l_j}\phi_j + \frac{\alpha-\alpha_{ij}}{l_j}\phi_{j+1}\right] d\alpha$$

$$-\int_{\alpha_{ij}}^{\alpha_{ij}+l_j} ln(r_{i\alpha})\left[\frac{\alpha_{ij}+l_j-\alpha}{l_j}\left(\frac{\partial \phi}{\partial n}\right)_j + \frac{\alpha-\alpha_{ij}}{l_j}\left(\frac{\partial \phi}{\partial n}\right)_{j+1}\right] d\alpha \tag{2.13}$$

or

$$A_{1ij}\phi_j + A_{2ij}\phi_{j+1} - B_{1ij}\left(\frac{\partial \phi}{\partial n}\right)_j - B_{2ij}\left(\frac{\partial \phi}{\partial n}\right)_{j+1} \tag{2.14}$$

where, for non singular case ($j \neq i-1$ or $j \neq i$)

$$A_{1ij} = \frac{\beta_{ij}}{l_j}\left[(\alpha_{ij}+l_j)\int_{\alpha_{ij}}^{\alpha_{ij}+l_j} \frac{1}{\beta_{ij}^2+\alpha^2} d\alpha - \int_{\alpha_{ij}}^{\alpha_{ij}+l_j} \frac{\alpha}{\beta_{ij}^2+\alpha^2} d\alpha\right] \tag{2.15a}$$

or

$$A_{1ij} = \frac{\alpha_{ij}+l_j}{l_j}\left[tan^{-1}\left(\frac{\alpha_{ij}+l_j}{\beta_{ij}}\right) - tan^{-1}\left(\frac{\alpha_{ij}}{\beta_{ij}}\right)\right] - \frac{\beta_{ij}}{2l_j} ln \frac{\beta_{ij}^2+\alpha_{ij}+{l_j}^2}{\beta_{ij}^2+\alpha_{ij}^2} \tag{2.15b}$$

$$A_{2ij} = \frac{\beta_{ij}}{l_j}\int_{\alpha_{ij}}^{\alpha_{ij}+l_j} \frac{\alpha}{\beta_{ij}^2+\alpha^2} d\alpha - \frac{\beta_{ij}}{l_j}\cdot\alpha_{ij}\int_{\alpha ij}^{\alpha_{ij}+l_j} \frac{1}{\beta_{ij}^2+\alpha^2} d\alpha \tag{2.16a}$$

or

$$A_{2ij} = -\frac{\alpha_{ij}}{l_j}\left[tan^{-1}\left(\frac{\alpha_{ij}+l_j}{\beta_{ij}}\right) - tan^{-1}\left(\frac{\alpha_{ij}}{\beta_{ij}}\right)\right] + \frac{\beta_{ij}}{2l_j} ln \frac{\beta_{ij}^2+\alpha_{ij}+{l_j}^2}{\beta_{ij}^2+\alpha_{ij}^2} \tag{2.16b}$$

$$B_{1ij} = \frac{\alpha_{ij} + l_j}{l_j} \int_{\alpha_{ij}}^{\alpha_{ij}+l_j} ln(r_{i\alpha}) d\alpha - \frac{1}{l_j} \int_{\alpha_{ij}}^{\alpha_{ij}+l_j} \alpha ln(r_{i\alpha}) d\alpha \qquad (2.17a)$$

or

$$B_{1ij} = \frac{\alpha_{ij} + l_j}{l_j} \left[\alpha_{ij} ln \frac{r_{i,j+1}}{r_{i,j}} + l_j \left\{ ln(r_{i,j+1}) - 1 \right\} + \beta_{ij} \left\{ tan^{-1} \left(\frac{\alpha_{ij} + l_j}{\beta_{ij}} \right) \right. \right.$$

$$\left. \left. - tan^{-1} \left(\frac{\alpha_{ij}}{\beta_{ij}} \right) \right\} \right] - \frac{1}{4l_j} \left[r_{i,j+1}^2 \left(2ln(r_{i,j+1}) - 1 \right) - r_{i,j}^2 \left(2ln(r_{i,j}) - 1 \right) \right] \qquad (2.17b)$$

$$B_{2ij} = \int_{\alpha_{ij}}^{\alpha_{ij}+l_j} ln(r_{i\alpha}) \frac{\alpha - \alpha_{ij}}{l_j} d\alpha \qquad (2.18a)$$

or

$$B_{2ij} = -\frac{\alpha_{ij}}{l_j} \left[\alpha_{ij} ln \frac{r_{i,j+1}}{r_{i,j}} + l_j \left\{ ln(r_{i,j+1}) - 1 \right\} + \beta_{ij} \left\{ tan^{-1} \left(\frac{\alpha_{ij} + l_j}{\beta_{ij}} \right) \right. \right.$$

$$\left. \left. - tan^{-1} \left(\frac{\alpha_{ij}}{\beta_{ij}} \right) \right\} \right] - \frac{1}{4l_j} \left[r_{i,j+1}^2 \left(2ln(r_{i,j+1}) - 1 \right) - r_{i,j}^2 \left(2ln(r_{i,j}) - 1 \right) \right] \qquad (2.18b)$$

and for singular case (j=i and j=i-1) as shown in Figure 2.4

$$\int_\Gamma \left(\frac{\phi}{r} \frac{\partial r}{\partial n} - ln(r) \frac{\partial \phi}{\partial n} \right) dS = \int_{l_{i-1}}^{0} \frac{\phi}{r} \frac{\partial r}{\partial n} (-dr) + \int_0^{l_i} \frac{\phi}{r} \frac{\partial r}{\partial n} dr$$

$$- \int_{l_{i-1}}^{0} ln(r) \frac{\partial \phi}{\partial n} (-dr) - \int_0^{l_i} ln(r) \frac{\partial \phi}{\partial n} dr \qquad (2.19)$$

Since r is perpendicular to $\hat{n}$, $\frac{\partial r}{\partial n} = 0$ for both elements (i-1, i) and also $lim_{r \to 0} \frac{1}{r} \frac{\partial r}{\partial n} = 0$, first two integrals of the equation are vanished. Thus Equation 2.19 becomes

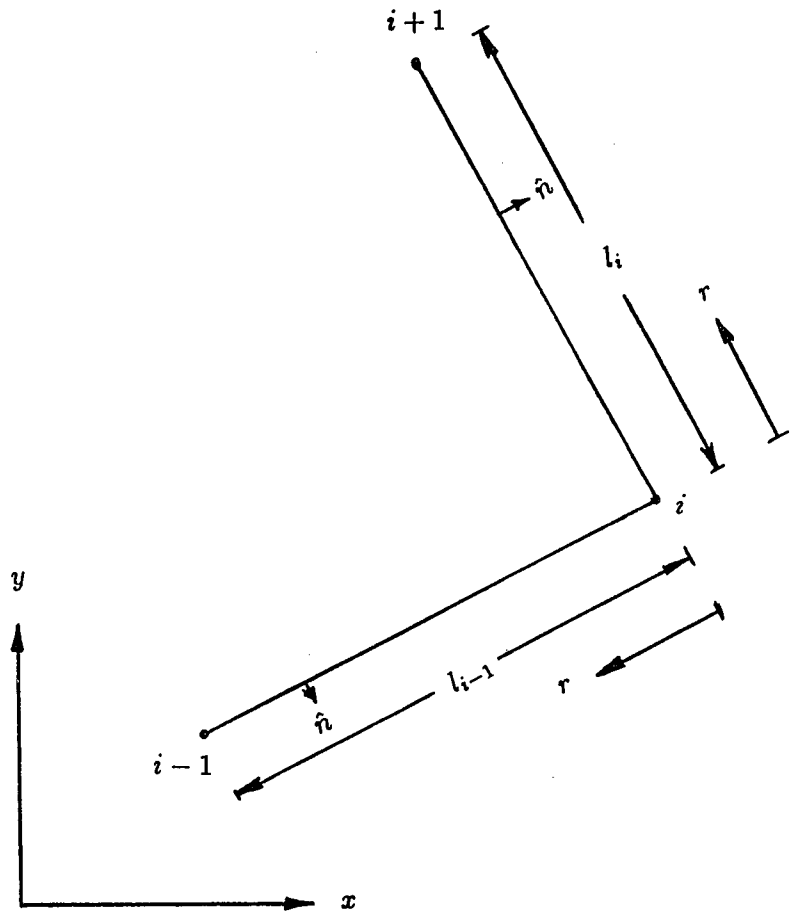

Figure 2.4. coordinate system (Singular case)

$$-\left[\int_0^{l_{i-1}} ln(r)\frac{\partial\phi}{\partial n}dr + \int_0^{l_i} ln(r)\frac{\partial\phi}{\partial n}dr\right] = -\int_0^{l_{i-1}} \frac{r}{l_{i-1}} ln(r)\left(\frac{\partial\phi}{\partial n}\right)_{i-1} dr$$
$$-\int_0^{l_{i-1}} \frac{l_{i-1}-r}{l_{i-1}} ln(r)\left(\frac{\partial\phi}{\partial n}\right)_{i} dr - \int_0^{l_i} \frac{r}{l_i} ln(r)\left(\frac{\partial\phi}{\partial n}\right)_{i+1} dr$$
$$-\int_0^{l_i} \frac{l_i-r}{l_i} ln(r)\left(\frac{\partial\phi}{\partial n}\right)_{i} dr \qquad (2.20a)$$

or

$$-\left[\int_0^{l_{i-1}} ln(r)\frac{\partial\phi}{\partial n}dr + \int_0^{l_i} ln(r)\frac{\partial\phi}{\partial n}dr\right] = -\frac{l_{i-1}}{4}\left(2ln(l_{i-1})-1\right)\left(\frac{\partial\phi}{\partial n}\right)_{i-1}$$
$$-\frac{l_{i-1}}{4}\left(2ln(l_{i-1})-3\right)\left(\frac{\partial\phi}{\partial n}\right)_{i} - \frac{l_i}{4}\left(2ln(l_i)-1\right)\left(\frac{\partial\phi}{\partial n}\right)_{i+1} - \frac{l_i}{4}\left(2ln(l_j)-3\right)\left(\frac{\partial\phi}{\partial n}\right)_{i} \qquad (2.20b)$$

Therefore,

$$j = i-1, \quad A_{1ij} = A_{2ij} = 0; \quad B_{1ij} = \frac{l_j}{4}\left(2ln(l_j)-1\right); \quad B_{2ij} = \frac{l_j}{4}\left(2ln(l_j)-3\right) \qquad (2.21)$$

$$j = i, \quad A_{1ij} = A_{2ij} = 0; \quad B_{1ij} = \frac{l_j}{4}\left(2ln(l_j)-3\right); \quad B_{2ij} = \frac{l_j}{4}\left(2ln(l_j)-1\right) \qquad (2.22)$$

Finally, Equation 2.11 can be written as,

$$\sum_{j=1}^{N} L_{ij}\phi_j = \sum_{j=1}^{N} R_{ij}\left(\frac{\partial\phi}{\partial n}\right)_j \qquad (2.23)$$

Where, $L_{ij} = A_{2ij}$ (previous element) + A_{1ij} (following element) - $\delta_{ij}c_i$ and $R_{ij} = B_{2ij}$ (previous element) + B_{1ij} (following element) in which $\delta_{ij} = 0$ for $i \neq j$ and $\delta_{ij} = 1$ for i = j. By moving the source point around the boundary, i.e., i = 1 to N, the following matrix equation is obtained

$$[L]\{\phi\} = [R]\left\{\frac{\partial\phi}{\partial n}\right\} \qquad (2.24)$$

where

$$\{\phi\} = [\phi_1, \phi_2, ...\phi_N]^T$$

and

$$\left\{\frac{\partial\phi}{\partial n}\right\} = \left[\left\{\frac{\partial\phi}{\partial n}\right\}_1, \left\{\frac{\partial\phi}{\partial n}\right\}_2, ... \left\{\frac{\partial\phi}{\partial n}\right\}_N\right]^T$$

Out of 2N values for ϕ & $\frac{\partial\phi}{\partial n}$, N values will be known from the boundary conditions for a given problem. Equation 2.24 can then be solved for the other N values and Equation 2.9 can be used to calculate the potential at internal points. The boundary conditions as required for the solution of the N values are as follows.

Along the upstream and downstream reservoir surface, potentials are given by

$$\phi = h_1 \tag{2.25}$$

$$\phi = h_2 \tag{2.26}$$

Where h_1 and h_2 are equal to the heights of the water level of the upstream and downstream reservoirs respectively (Dirichlet condition). For impervious layer, normal derivative of the potential is zero i.e.

$$\frac{\partial\phi}{\partial n} = 0 \tag{2.27}$$

This means there is no flow through impervious layer (Neuman condition). Along seepage surface, potential is equal to the vertical elevation, y, i.e.

$$\phi = y \tag{2.28}$$

For unsteady flow, the boundary condition of the free surface is

$$\phi = \eta \tag{2.29}$$

Where η represents the vertical location of the free surface which is a function of horizontal distance, x and the time ,t. But for porous media, since the free surface is a material surface, the rate of change of the position of the free surface is equal to vertical velocity on the free surface, i.e.

$$-\frac{\partial \eta}{\partial t} + \frac{q}{n} \cdot \nabla(z - \eta) = 0 \tag{2.30}$$

In which q is the specific discharge and n is the porosity. If the unit vector is defined as

$$\hat{n} = \frac{\nabla(z - \eta)}{|\nabla(z - \eta)|}$$

the above equation can be written in the following form.

$$\frac{\partial \eta}{\partial t} = \frac{q}{n} \cdot \hat{n} |\nabla(z - \eta)| \tag{2.31}$$

Substituting

$$|\nabla(z - \eta)| = \left[1 + \left(\frac{\partial \eta}{\partial x}\right)^2\right]^{\frac{1}{2}}$$

and

$$q = -k \nabla \phi$$

the above equation follows

$$\frac{\partial \eta}{\partial t} = -\frac{k}{n}\left[1 + \left(\frac{\partial \eta}{\partial x}\right)^2\right]^{\frac{1}{2}} \nabla \phi \cdot \hat{n} \tag{2.32}$$

or

$$\frac{\partial \eta}{\partial t} = -\frac{k}{n}\left[1 + \left(\frac{\partial \eta}{\partial x}\right)^2\right]^{\frac{1}{2}} \frac{\partial \phi}{\partial n} \tag{2.33}$$

Assuming a dimensionless time, t_D such that

$$t_D = \frac{tk}{nL}$$

where t is the real time, k is the hydraulic conductivity and L is the characteristic length scale, then the Equation 2.33 becomes

$$\frac{\partial \eta}{\partial t} = -\left[1 + \left(\frac{\partial \eta}{\partial x}\right)^2\right]^{\frac{1}{2}} \frac{\partial \phi}{\partial n} \tag{2.34}$$

or

$$\left(\frac{\partial \phi}{\partial t}\right)_x = -\left(1 + tan^2\beta\right)^{\frac{1}{2}} \frac{\partial \phi}{\partial n} \tag{2.35}$$

Where β is the angle between the free surface profile and the x-axis as shown in Figure 2.5, such that $\frac{\partial \eta}{\partial x} = -tan\beta$ and $\phi = \eta$. Alternately the Equation 2.33 can be written as

$$\left(\frac{\partial \phi}{\partial t}\right)_x = -\frac{1}{cos\beta} \frac{\partial \phi}{\partial n} \tag{2.36}$$

In finite difference form using a weighting factor of θ for $t + \Delta t$, the Equation 2.36 is as follows

$$\frac{\phi_{t+\Delta t} - \phi_t}{\Delta t} = -\frac{1}{cos\beta}\left[\theta\left(\frac{\partial \phi}{\partial n}\right)_{t+\Delta t} + (1-\theta)\left(\frac{\partial \phi}{\partial n}\right)_t\right] \tag{2.37}$$

or

$$\phi_{t+\Delta t} = \phi_t - \frac{\Delta t}{cos\beta}\left[\theta\left(\frac{\partial \phi}{\partial n}\right)_{t+\Delta t} + (1-\theta)\left(\frac{\partial \phi}{\partial n}\right)_t\right] \tag{2.38}$$

Equation 2.38 indicates that, if ϕ and $\frac{\partial \phi}{\partial n}$ is known at time t then ϕ and $\frac{\partial \phi}{\partial n}$ can be computed at time $t + \Delta t$ on the free surface.

As mentioned earlier, the potential for internal point is calculated from Equation 2.9 which, for $c = 2\pi$, becomes as

$$2\pi\phi_i = \int_\Gamma \left(\frac{\phi}{r}\frac{\partial r}{\partial n} - ln(r)\frac{\partial \phi}{\partial r}\right) ds \tag{2.39}$$

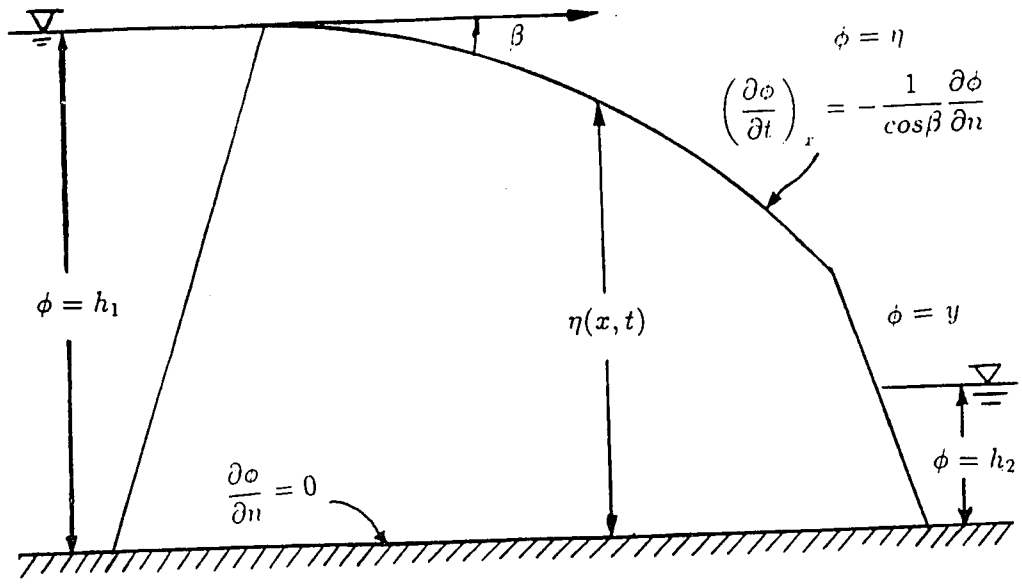

Figure 2.5. Boundary conditions for an unsteady state flow through an earthen dam

where i is the internal point as shown in Figure 2.6. And the derivatives of the potential in x and y directions are as follows

$$\left(\frac{\partial\phi}{\partial x}\right)_i = \frac{1}{2\pi}\int_\Gamma \left[\phi\frac{\partial}{\partial x}\left(\frac{1}{r}\frac{\partial r}{\partial n}\right) - \frac{\partial\phi}{\partial n}\frac{\partial}{\partial x}\Big(ln(r)\Big)\right]ds \tag{2.40}$$

$$\left(\frac{\partial\phi}{\partial y}\right)_i = \frac{1}{2\pi}\int_\Gamma \left[\phi\frac{\partial}{\partial y}\left(\frac{1}{r}\frac{\partial r}{\partial n}\right) - \frac{\partial\phi}{\partial n}\frac{\partial}{\partial y}\Big(ln(r)\Big)\right]ds \tag{2.41}$$

Finally, upon integration, Equation 2.40 and 2.41 becomes

$$\left(\frac{\partial\phi}{\partial x}\right)_i = \frac{1}{2\pi}\left[\sum_{j=1}^{N} A_{xj}\phi_j + A_{xj1}\phi_{j+1} + B_{xj}\left(\frac{\partial\phi}{\partial n}\right)_j + B_{xj1}\left(\frac{\partial\phi}{\partial n}\right)_{j+1}\right] \tag{2.42}$$

$$\left(\frac{\partial\phi}{\partial y}\right)_i = \frac{1}{2\pi}\left[\sum_{j=1}^{N} A_{yj}\phi_j + A_{yj1}\phi_{j+1} + B_{yj}\left(\frac{\partial\phi}{\partial n}\right)_j + B_{yj1}\left(\frac{\partial\phi}{\partial n}\right)_{j+1}\right] \tag{2.43}$$

where

$$\begin{aligned} A_{xj} = &-\frac{\beta_{ij}}{l_j}\Big\{\Big(\alpha_{ij}+l_j\Big)cos\theta - \beta_{ij}sin\theta\Big\}\left(\frac{1}{r_{i,j+1}^2} - \frac{1}{r_{i,j}^2}\right) \\ &+\frac{1}{l_j}\Big\{\Big(\alpha_{ij}+l_j\Big)sin\theta + \beta_{ij}cos\theta\Big\}\left(\frac{\alpha_{ij}+l_j}{r_{i,j+1}} - \frac{\alpha_{ij}}{r_{i,j}}\right) + \frac{sin\theta}{l_j}ln\frac{r_{i,j+1}}{r_{i,j}} \\ &-\frac{cos\theta}{l_j}\left\{tan^{-1}\frac{\alpha_{ij}+l_j}{\beta_{ij}} - tan^{-1}\frac{\alpha_{ij}}{\beta_{ij}}\right\} \end{aligned} \tag{2.44}$$

$$\begin{aligned} A_{xj1} = &\frac{\beta_{ij}}{l_j}\Big\{\alpha_{ij}cos\theta - \beta_{ij}sin\theta\Big\}\left(\frac{1}{r_{i,j+1}^2} - \frac{1}{r_{i,j}^2}\right) \\ &-\frac{1}{l_j}\Big\{\alpha_{ij}sin\theta + \beta_{ij}cos\theta\Big\}\left(\frac{\alpha_{ij}+l_j}{r_{i,j+1}} - \frac{\alpha_{ij}}{r_{i,j}}\right) - \frac{sin\theta}{l_j}ln\frac{r_{i,j+1}}{r_{i,j}} \\ &+\frac{cos\theta}{l_j}\left\{tan^{-1}\frac{\alpha_{ij}+l_j}{\beta_{ij}} - tan^{-1}\frac{\alpha_{ij}}{\beta_{ij}}\right\} \end{aligned} \tag{2.45}$$

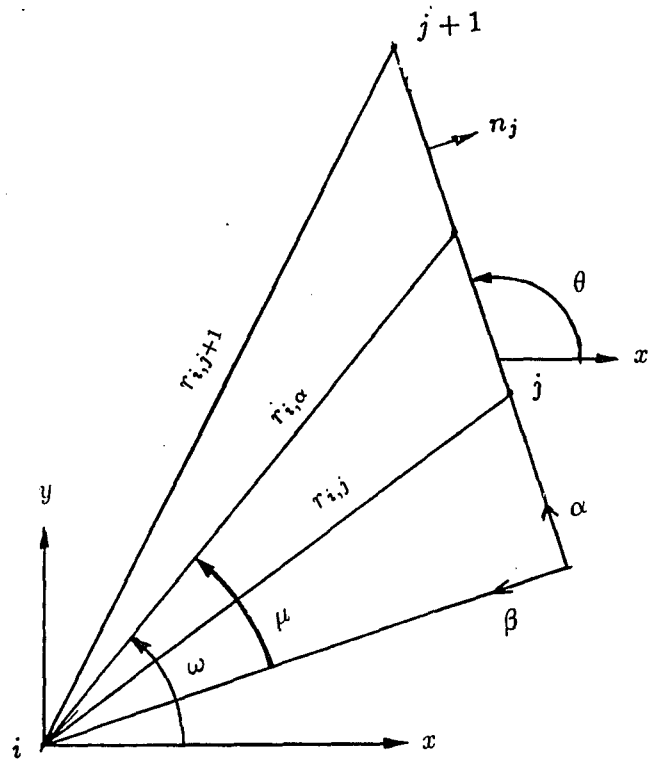

Figure 2.5. Definition sketch for the interior solution

$$B_{xj} = \frac{\alpha_{ij}+l_j}{l_j} sin\theta \left\{ tan^{-1}\frac{\alpha_{ij}+l_j}{\beta_{ij}} - tan^{-1}\frac{\alpha_{ij}}{\beta_{ij}} \right\} + \left(\frac{\alpha_{ij}+l_j}{l_j} cos\theta \right.$$
$$\left. -\frac{\beta_{ij}}{l_j} sin\theta \right) ln\frac{r_{i,j+1}}{r_{i,j}} - \frac{cos\theta}{l_j} \left\{ l_j - \beta_{ij} \left(tan^{-1}\frac{\alpha_{ij}+l_j}{\beta_{ij}} - tan^{\frac{-1\alpha_{ij}}{\beta_{ij}}} \right) \right\} \qquad (2.46)$$

$$B_{xj1} = -\frac{\alpha_{ij}}{l_j} sin\theta \left\{ tan^{-1}\frac{\alpha_{ij}+l_j}{\beta_{ij}} - tan^{-1}\frac{\alpha_{ij}}{\beta_{ij}} \right\} - \left(\frac{\alpha_{ij}}{l_j} cos\theta \right.$$
$$\left. -\frac{\beta_{ij}}{l_j} sin\theta \right) ln\frac{r_{i,j+1}}{r_{i,j}} + \frac{cos\theta}{l_j} \left\{ l_j - \beta_{ij} \left(tan^{-1}\frac{\alpha_{ij}+l_j}{\beta_{ij}} - tan^{\frac{-1\alpha_{ij}}{\beta_{ij}}} \right) \right\} \qquad (2.47)$$

$$A_{yj} = \frac{\alpha_{ij}+l_j}{l_j} \left[-cos\theta \left(\frac{\alpha_{ij}+l_j}{r^2_{i,j+1}} - \frac{\alpha_{ij}}{r^2_{i,j}} \right) - \beta_{ij} sin\theta \left(\frac{1}{r^2_{i,j+1}} - \frac{1}{r^2_{i,j}} \right) \right]$$
$$-\frac{cos\theta}{l_j} ln\frac{r_{i,j+1}}{r_{i,j}} - \beta^2 \frac{cos\theta}{l_j} \left(\frac{1}{r^2_{i,j+1}} - \frac{1}{r^2_{i,j}} \right) + \frac{\beta_{ij} sin\theta}{l_j} \left(\frac{\alpha_{ij}+l_j}{r^2_{i,j+1}} - \frac{\alpha_{ij}}{r^2_{i,j}} \right)$$
$$-\frac{sin\theta}{l_j} \left(tan^{-1}\frac{\alpha_{ij}+l_j}{\beta_{ij}} - tan^{-1}\frac{\alpha_{ij}}{\beta_{ij}} \right) \qquad (2.48)$$

$$A_{yj1} = -\frac{\alpha_{ij}}{l_j} \left[-cos\theta \left(\frac{\alpha_{ij}+l_j}{r^2_{i,j+1}} - \frac{\alpha_{ij}}{r^2_{i,j}} \right) - \beta_{ij} sin\theta \left(\frac{1}{r^2_{i,j+1}} - \frac{1}{r^2_{i,j}} \right) \right]$$
$$+\frac{cos\theta}{l_j} ln\frac{r_{i,j+1}}{r_{i,j}} + \beta^2 \frac{cos\theta}{l_j} \left(\frac{1}{r^2_{i,j+1}} - \frac{1}{r^2_{i,j}} \right) - \frac{\beta_{ij} sin\theta}{l_j} \left(\frac{\alpha_{ij}+l_j}{r^2_{i,j+1}} - \frac{\alpha_{ij}}{r^2_{i,j}} \right)$$
$$+\frac{sin\theta}{l_j} \left(tan^{-1}\frac{\alpha_{ij}+l_j}{\beta_{ij}} - tan^{-1}\frac{\alpha_{ij}}{\beta_{ij}} \right) \qquad (2.49)$$

$$B_{yj} = \frac{\alpha_{ij}+l_j}{l_j} \left\{ sin\theta ln\frac{r_{i,j+1}}{r_{i,j}} - cos\theta \left(tan^{-1}\frac{\alpha_{ij}+l_j}{\beta_{ij}} - tan^{-1}\frac{\alpha_{ij}}{\beta_{ij}} \right) \right\}$$

$$-sin\theta + \frac{\beta_{ij}}{l_j} cos\theta ln \frac{r_{i,j+1}}{r_{i,j}} + \frac{\beta_{ij}}{l_j} sin\theta \left(tan^{-1} \frac{\alpha_{ij} + l_j}{\beta_{ij}} tan^{-1} \frac{\alpha_{ij}}{\beta_{ij}} \right) \tag{2.50}$$

$$B_{yj1} = -\frac{\alpha_{ij}}{l_j} \left\{ sin\theta ln \frac{r_{i,j+1}}{r_{i,j}} - cos\theta \left(tan^{-1} \frac{\alpha_{ij} + l_j}{\beta_{ij}} - tan^{-1} \frac{\alpha_{ij}}{\beta_{ij}} \right) \right\}$$
$$+sin\theta - \frac{\beta_{ij}}{l_j} cos\theta ln \frac{r_{i,j+1}}{r_{i,j}} - \frac{\beta_{ij}}{l_j} sin\theta \left(tan^{-1} \frac{\alpha_{ij} + l_j}{\beta_{ij}} tan^{-1} \frac{\alpha_{ij}}{\beta_{ij}} \right) \tag{2.51}$$

In the above expressions, $r_{i,j}$, $r_{i,j+1}$, β_{ij}, α_{ij} and l_j are evaluated from coordinates (x_i, y_i), (x_j, y_j), (x_{j+1}, y_{j+1}) as follows

$$\bar{r}_{i,j+1} = (x_{j+1} - x_i) \cdot \hat{p} + (y_{j+1} - y_i) \cdot \hat{q}$$

or

$$r_{i,j+1} = \left[(x_{j+1} - x_i)^2 - (y_{j+1} - y_i)^2 \right]^{\frac{1}{2}}$$

$$\bar{r}_{i,j} = (x_j - x_i) \cdot \hat{p} + (y_j - y_i) \cdot \hat{q}$$

or

$$r_{i,j} = \left[(x_j - x_i)^2 - (y_j - y_i)^2 \right]^{\frac{1}{2}}$$

$$l_j = \left[(x_{j+1} - x_j)^2 + (y_{j+1} - y_j)^2 \right]^{\frac{1}{2}}$$

$$\hat{n} = \frac{y_{j+1} - y_j}{l_j} \cdot \hat{p} - \frac{x_{j+1} - x_j}{l_j} \cdot \hat{q}$$

$$\hat{\beta} = -\hat{n} = -\frac{y_{j+1} - y_j}{l_j} \cdot \hat{p} + \frac{x_{j+1} - x_j}{l_j} \cdot \hat{q}$$

$$\hat{\alpha} = \frac{x_{j+1} - x_j}{l_j} \cdot \hat{p} + \frac{y_{j+1} - y_j}{l_j} \cdot \hat{q}$$

$$\beta_{ij} = \bar{r}_{i,j} \cdot \hat{n} = \frac{(x_j - x_i)(y_{j+1} - y_j)}{l_j} - \frac{(y_j - y_i)(x_{j+1} - x_j)}{l_j}$$

$$\alpha_{ij} = \bar{r}_{i,j} \cdot \hat{\alpha} = \frac{(x_j - x_i)(x_{j+1} - x_j)}{l_j} + \frac{(y_j - y_i)(y_{j+1} - y_j)}{l_j}$$

The above equations are used while developing a computer program for analysing unsteady flow through an earthen dam.

CHAPTER 3

NUMERICAL MODEL

The boundary integral method as discussed in the previous chapter has been used in this study to investigate the flow through an earthen dam. The provision for both rising and falling of upstream water level is considered in this study. In reality, in the case of falling head, a seepage surface, as shown in Figure 3.1, is developed at the upstream reservoir. Realizing this fact, a seepage surface provision at the upstream face has been implemented in the computer model. The algorithm of this model is described in the following

For a typical stage variation (Figure 3.1), when the upstream water level starts falling, this model considers seepage surface on the upstream boundary. Since additional seepage points are introduced to account for the seepage surface, the number of points on the boundary is more than the number of points on the boundary in the case of rising reservoir level as shown in Figure 3.2. The extent of the seepage surface increases continuously with the falling of the upstream water level. When the upstream water level starts rising from the point of lowest water level of a typical cycle, the extent of the seepage surface decreases. In the course of further rising, the magnitude of the seepage surface will becomes negligible (tolerance limit 0.01) at some time. When that happens all the seepage nodes are eliminated and the initial number of nodes in the model (no seepage surface at

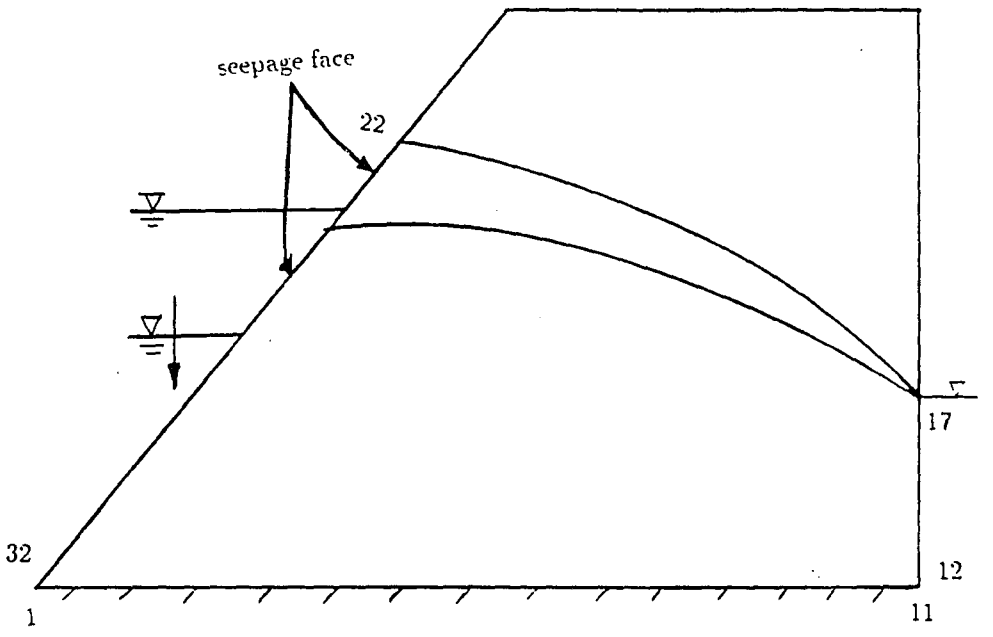

Figure 3.1. Number of nodes during falling of reservoir level

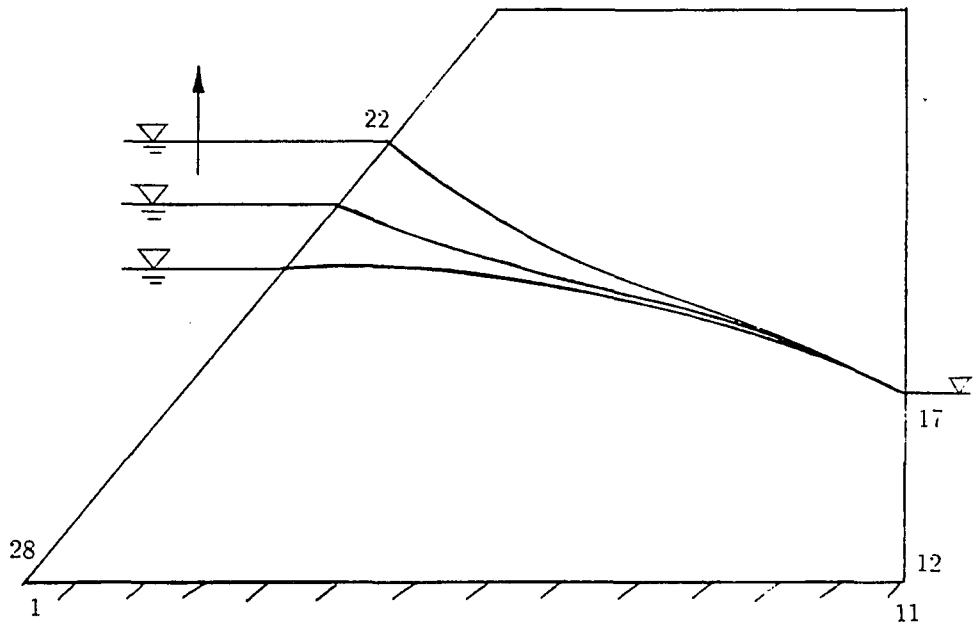

Figure 3.2. Number of nodes during rising of reservoir level

upstream) is obtained. Thus renumbering of the boundary nodes is necessary depending on the existence of seepage face at the upstream reservoir during any typical cycle of water level variation.

Two subroutines are developed in the computer program to include the seepage surface model at the upstream reservoir. The first subroutine determines whether a seepage surface exists. The second subroutine is used to renumber the nodes including specification of the type (code) of nodes (free surface node, seepage surface node etc.). The application of this model in analyzing a sample problem is presented in the following chapter.

CHAPTER 4

RESULTS OF APPLICATION AND DISCUSSION

4.1 General

A computer program was developed by the author using the integral equations as presented in Chapter 2. As mentioned in Chapter 3, the provision for seepage face at the upstream reservoir side is implemented in the computer program. Thus the program is capable of handling unsteady flow with falling head. The program is then used to show the application of BEM for solving potential problem such as a Colorado river beach at Grand Canyon where the boundary pressure and internal pressure variation at different points are determined due to the variation of upstream water levels. The results of these analyses are then compared with the available field results.

4.2 Beach model

To illustrate the use of this program, a beach along the Colorado river is analysed to determine the pressure or potential variation at phreatic surface and internal pressure at different points. Figure 4.1 shows the profile of a sandy beach along the Colorado river in the Grand Canyon. The corresponding numerical model of the beach considered for this study is shown in Figure 4.2. The beach has slopes of 1:6 and 1:1.5 at the upstream and downstream sides respectively. It is assumed

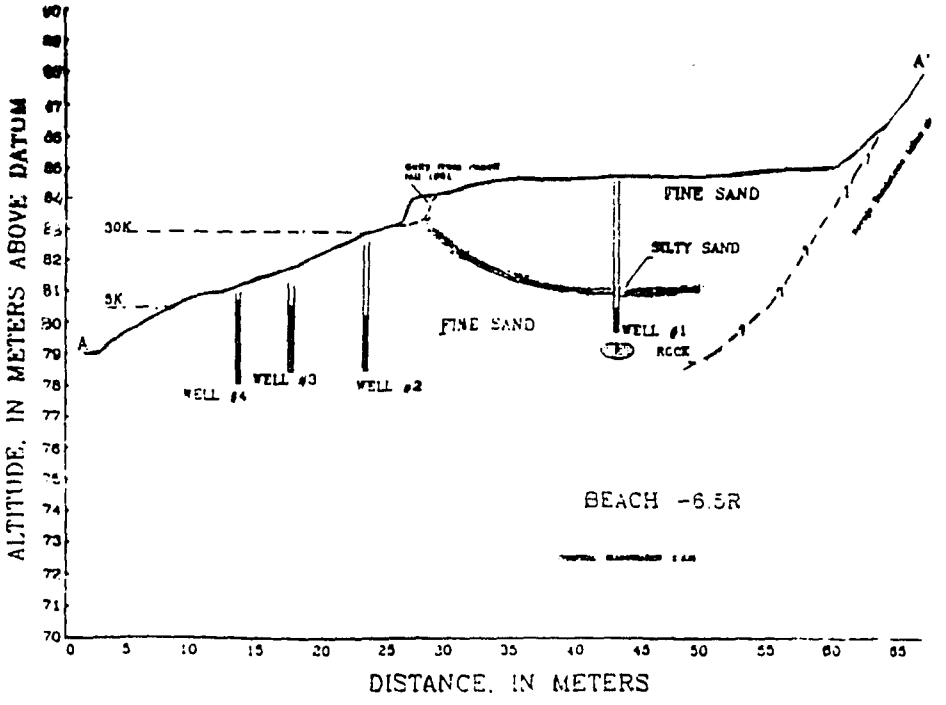

Figure 4.1. Profile of Grand Canyon beach

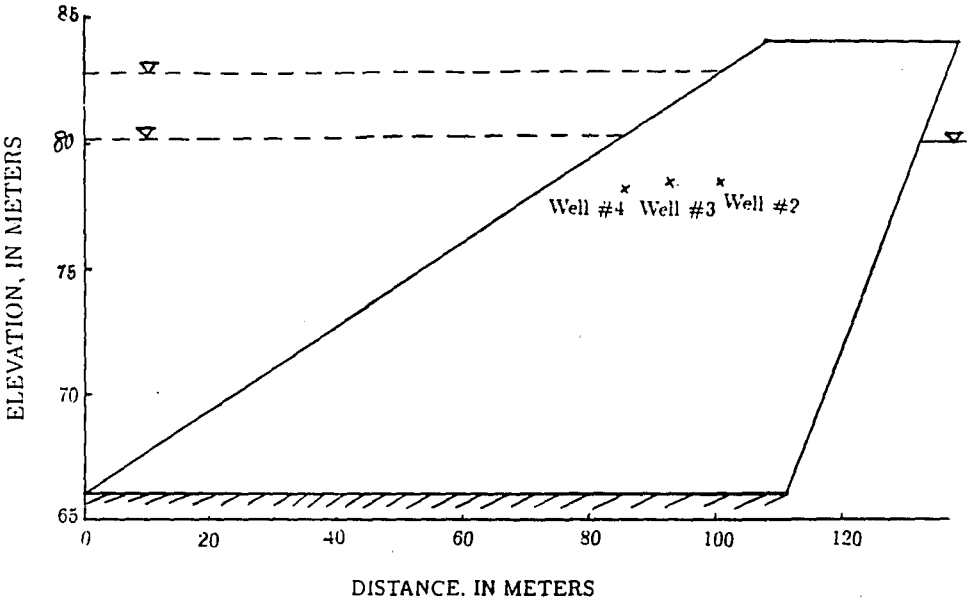

Figure 4.2. Beach model as used in this study for BEM analysis

that, there is an impervious layer of 110 meters in length at an elevation of 66 meters, and a constant head on the downstream side which is always equal to the lowest level of the upstream head for any type of stage variation. All these analyses are performed for two different five-days stage variation as observed in the Colorado river. These stage variations (Flow E & Flow G) are shown in Figures 4.3 and 4.4. The values for the hydraulic conductivity, k and the porosity, n, are considered to be 0.823m/hr. and 0.43 respectively.

4.3 Results and Discussion

4.3.1 Variation of phreatic surface within beach

The variation of the phreatic surface within the beach during a typical cycle is presented in Figure 4.5 and Figure 4.6 for the Flow E and Flow G respectively. As can be seen from Figure 4.5 when the upstream water level goes to the highest point of the cycle of stage variation, the phreatic surface rises accordingly on the upstream side. But there is no change of phreatic surface at the downstream side. On the other hand, when the upstream water level is at the lowest point of the cycle, the part of the phreatic surface is higher than that of the upstream water level. This is due to the slow movement of the water inside the dam than compared with that of the water level in the river. Thus between the river water level and the phreatic surface, a seepage face is formed. Upon rising from the lowest level, (Figure 4.5) this seepage face still exists but the extent of the seepage face is reduced as the phreatic surface shows a tendency to fall (downward direction of flow of water on the phreatic surface). At one moment, the water level of the upstream reservoir and the phreatic surface becomes same and the existence of the seepage surface is eliminated. After that the phreatic surface rises with the rising of upstream water

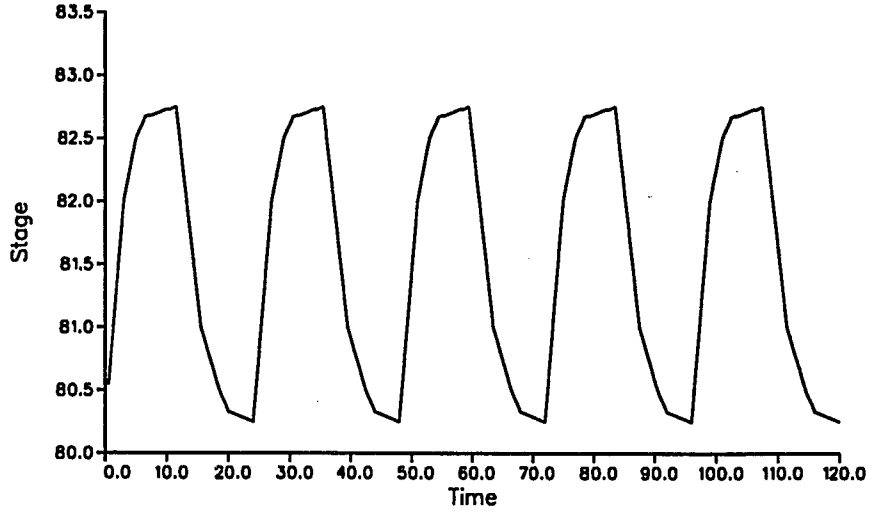

Figure 4.3. Stage variation in Colorado river (Flow E)

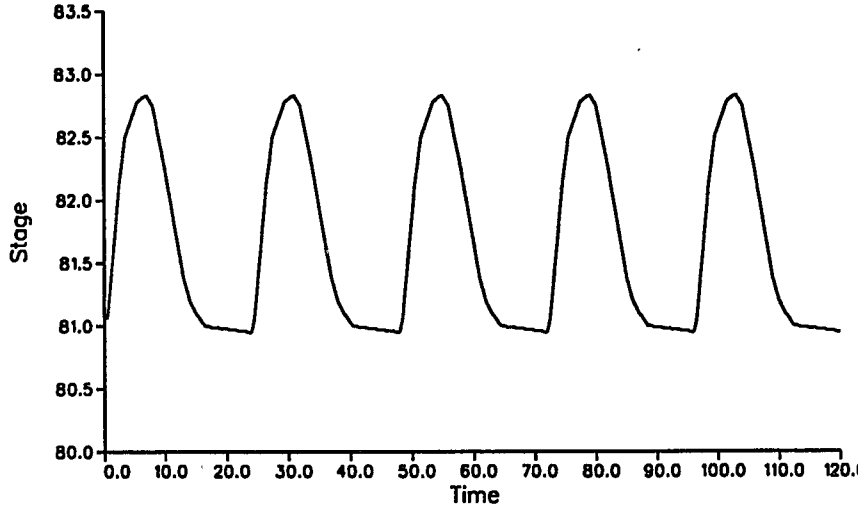

Figure 4.4. Stage variation in Colorado river (Flow G)

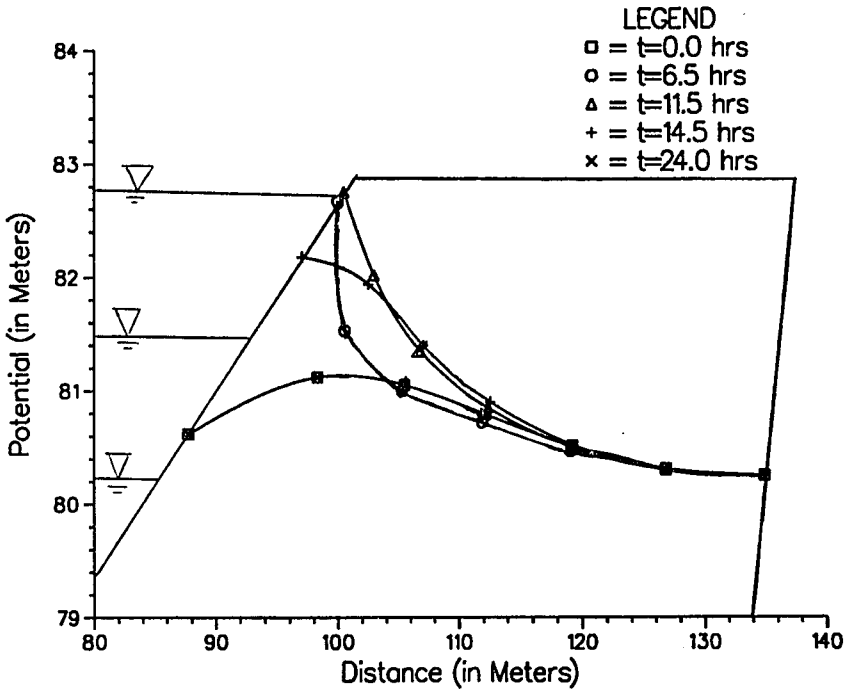

Figure 4.5. Phreatic surface variation within beach (Flow E)

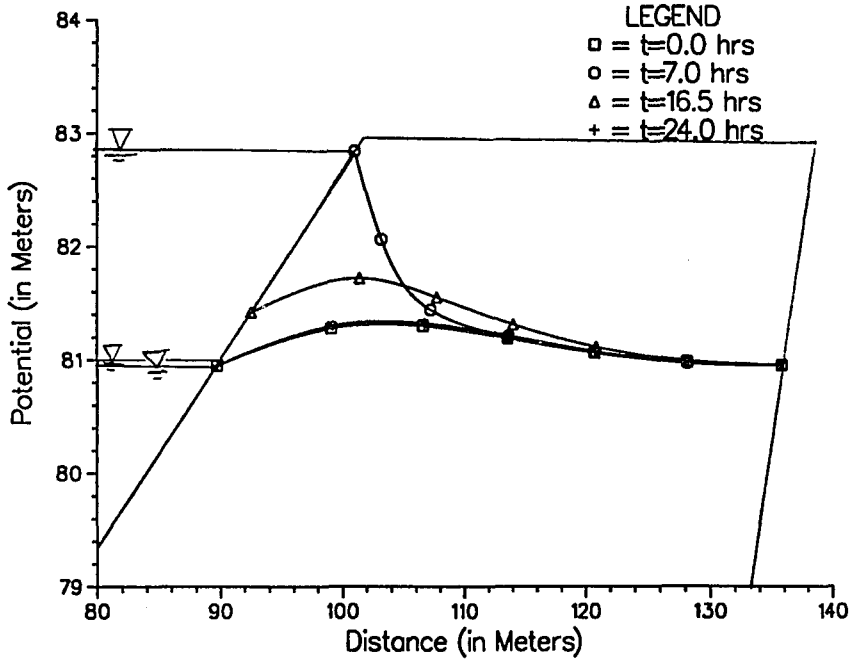

Figure 4.6. Phreatic surface variation within beach (Flow G)

level. But the position of the phreatic surface near the downstream face remains same as before. This behavior of the phreatic surface indicates that the pressure variation of the phreatic surface occurs significantly in the region near the river.

In the case, as shown in Figure 4.6 (Flow G), when the rate of falling of the upstream water level is lower than that of the phreatic surface, the extent of the seepage surface is reduced such that at one moment both the upstream water level and the phreatic surface reaches on the same level during the course of falling. After that both the level falls simultaneously such that there is no gap between them up to the lowest point of the cycle.

4.3.2Potential along base

For Flow E & Flow G, the change of potential or pressure at the base (impervious layer) for a typical cycle is illustrated in Figures 4.7 and 4.8. From these figures, it is observed that the pressure at the upstream side of the base varies accordingly with the variation of the upstream water level. In other words, the pressure at the upstream side of the base is dependent upon the position of the phreatic surface. The potential at the downstream face remains constant as observed for the phreatic surface. But when the water level on the upstream face approaches to the lowest point of the cycle, the middle portion of the impervious base experiences a higher pressure or potential compared to the sides of the base. This is due to the fact that, during falling the water inside the dam moves vertically downward and hits the impervious base. After hitting the impervious layer, the water turns its direction of movement both towards the upstream and downstream

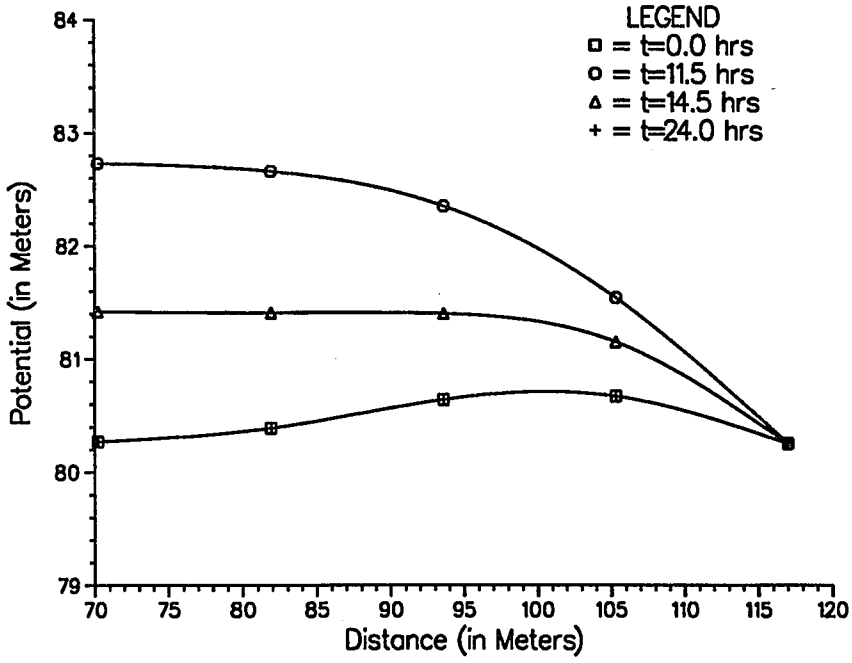

Figure 4.7. Potential along impervious base (Flow E)

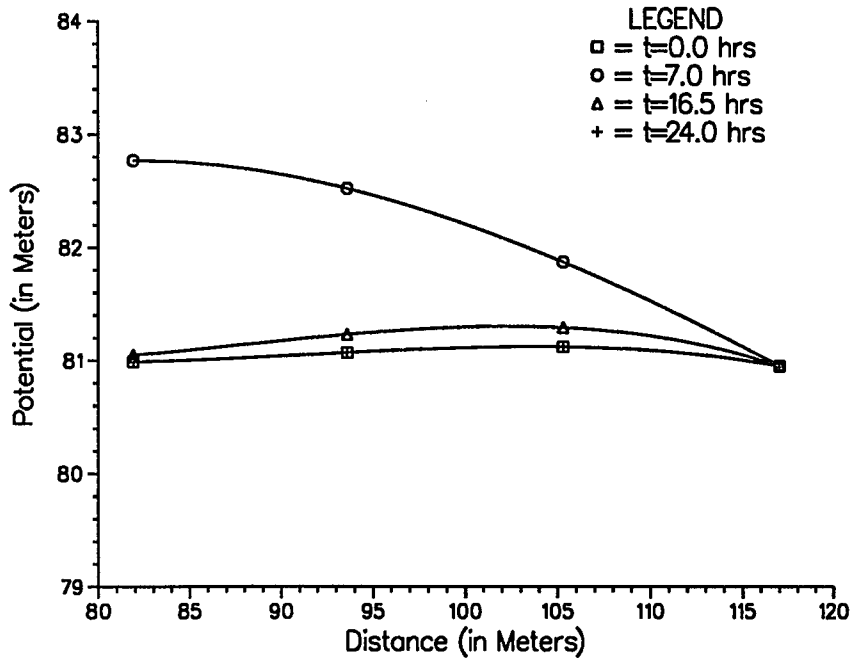

Figure 4.8. Potential along impervious base (Flow G)

faces to flow out from the dam. But in the middle the water experiences obstacle due to impervious layer and thus does not get any access to relieve the pressure.

4.3.3 Comparison of computations with field data

To demonstrate how the results of this method (BEM) compares with the actual measured data, the potential at different internal points of the Grand canyon beach are calculated for the two different stage variations as considered earlier. The results at these internal points are presented in Figure 4.9 to Figure 4.12. The experimental results (Appendix 1) for these are also shown in the figures for comparison with the BEM solutions. It can be observed from these figures that the potentials as obtained using the BEM agree well with the experiment. This comparison demonstrates that the BEM is a very good direct approach to find out the time dependent potential flow through porous media.

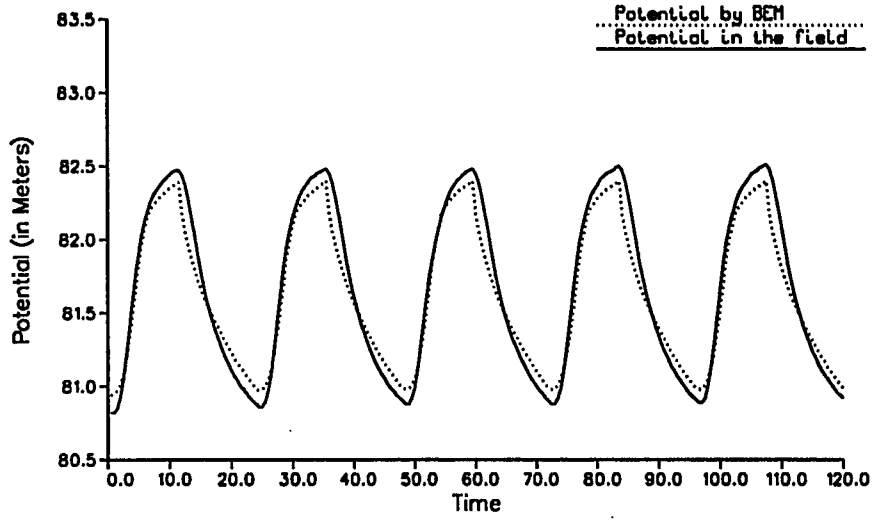

Figure 4.9. Potential vs. time at well 2 (Flow E)

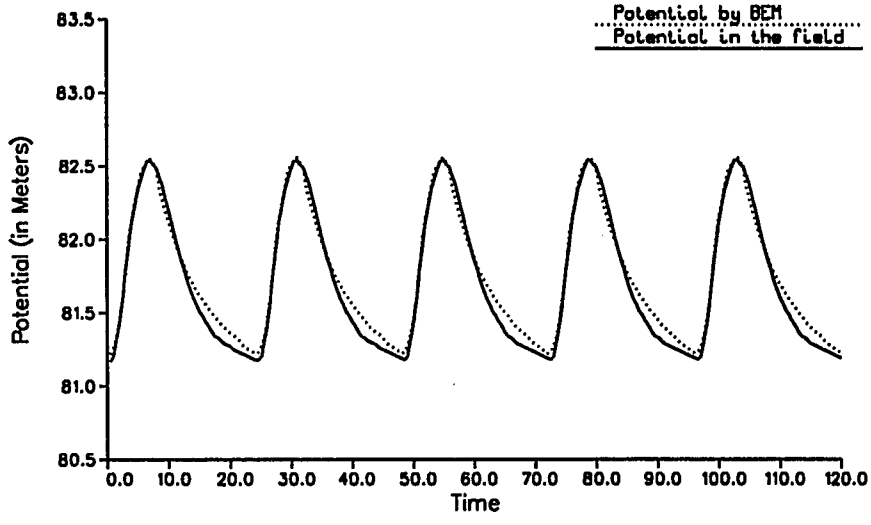

Figure 4.10. Potential vs. time at well 2 (Flow G)

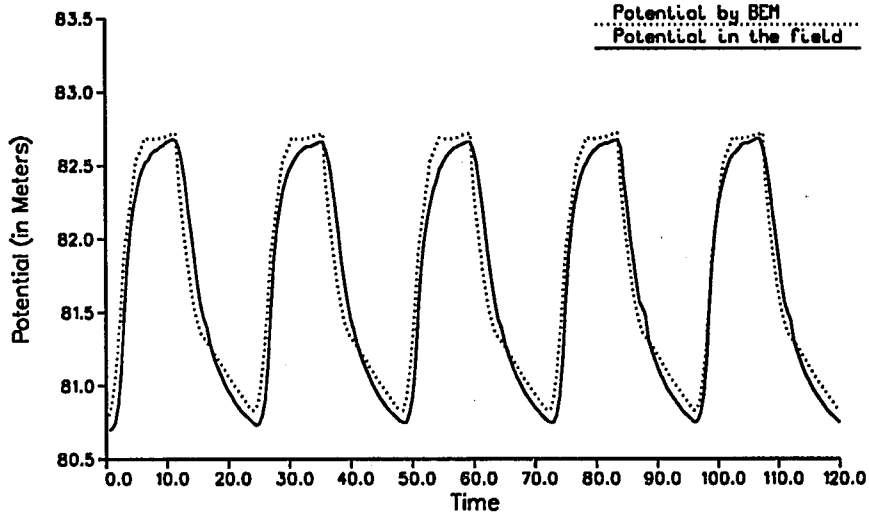

Figure 4.11. Potential vs. time at well 3 (Flow E)

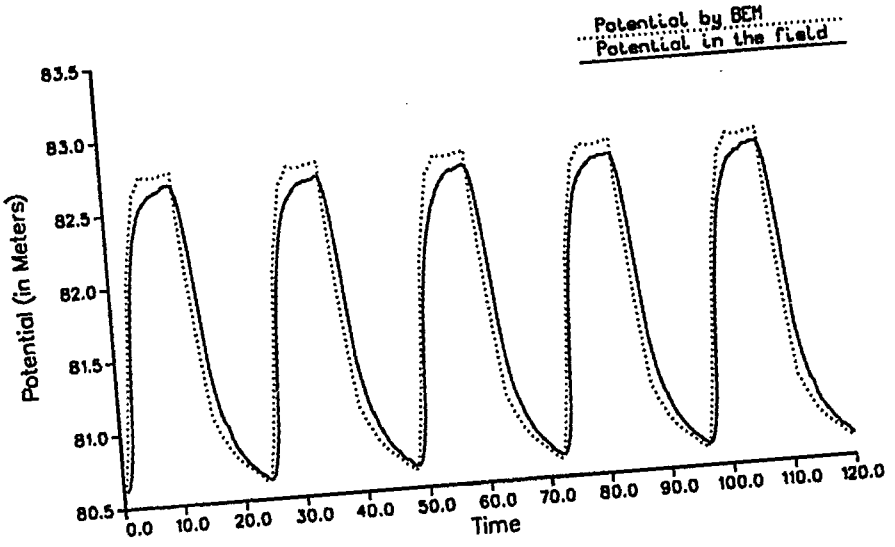

Figure 4.12. Potential vs. time at well 4 (Flow E)

CHAPTER 5

CONCLUSIONS

Based on the analyses performed in this study, the following conclusions can be drawn.

1. The boundary element method is a direct approach which can account for the seepage surface at both the upstream and downstream face as expected in the field.

2. This method gives boundary pressure as well as internal pressure directly and easily

3. The results as obtained in this study using BEM are in excellent agreement with those of field data.

4. A marked variation of pressure or potential is observed in the region near the upstream face of the beach with respect to stage variation.

APPENDIX A

Appendix 1: The 5 days stage variation in Colorado river and the potential variation at different wells in Grand Canyon beach

Time (hrs.)	Stage in Colorado river (meter)	Potential at well #2 (meter)	Potential at well #3 (meter)	Potential at well #4 (meter)
0.50	80.29	80.82	80.70	80.62
1.00	80.49	80.82	80.71	80.64
1.50	80.78	80.85	80.75	80.74
2.00	81.15	80.93	80.87	80.93
2.50	81.55	81.06	81.10	81.38
3.00	81.87	81.22	81.50	81.73
3.50	82.12	81.41	81.83	82.00
4.00	82.30	81.59	82.05	82.18
4.50	82.42	81.77	82.21	82.32
5.00	82.49	81.91	82.31	82.40
5.50	82.57	82.04	82.41	82.48
6.00	82.62	82.13	82.47	82.53
6.50	82.64	82.20	82.52	82.56
7.00	82.66	82.26	82.54	82.58
7.50	82.68	82.31	82.58	82.61
8.00	82.69	82.34	82.60	82.62
8.50	82.70	82.37	82.61	82.63
9.00	82.71	82.40	82.63	82.64
9.50	82.72	82.42	82.64	82.65
10.0	82.74	82.44	82.66	82.67
10.5	82.75	82.46	82.67	82.68
11.0	82.74	82.47	82.68	82.68
11.5	82.75	82.47	82.67	82.67
12.0	82.67	82.44	82.62	82.61
12.5	82.57	82.38	82.52	82.52
13.0	82.42	82.28	82.39	82.37
13.5	82.23	82.16	82.19	82.20
14.0	82.01	82.05	82.04	82.00
14.5	81.78	81.92	81.86	81.80
15.0	81.55	81.80	81.69	81.59

Appendix 1 (Continued)

Time (hrs.)	Stage in Colorado river (meter)	Potential at well #2 (meter)	Potential at well #3 (meter)	Potential at well #4 (meter)
15.5	81.33	81.69	81.55	81.41
16.0	81.13	81.59	81.46	81.29
16.5	80.95	81.51	81.40	81.19
17.0	80.80	81.43	81.29	81.10
17.5	80.68	81.37	81.21	81.04
18.0	80.58	81.31	81.15	81.01
18.5	80.49	81.25	81.10	80.93
19.0	80.43	81.20	81.05	80.88
19.5	80.38	81.15	81.00	80.84
20.0	80.35	81.11	80.96	80.81
20.5	80.33	81.07	80.93	80.78
21.0	80.31	81.04	80.89	80.75
21.5	80.29	81.00	80.86	80.73
22.0	80.29	80.98	80.83	80.71
22.5	80.28	80.95	80.81	80.69
23.0	80.28	80.92	80.79	80.67
23.5	80.27	80.90	80.76	80.66
24.0	80.27	80.88	80.75	80.64
24.5	80.33	80.86	80.73	80.63
25.0	80.49	80.86	80.74	80.66
25.5	80.78	80.90	80.79	80.77
26.0	81.14	80.98	80.90	80.95
26.5	81.54	81.10	81.14	81.38
27.0	81.86	81.27	81.53	81.72
27.5	82.11	81.45	81.86	81.98
28.0	82.27	81.63	82.07	82.15
28.5	82.40	81.81	82.21	82.29
29.0	82.49	81.95	82.33	82.39
29.5	82.55	82.06	82.41	82.46
30.0	82.59	82.15	82.47	82.51
30.5	82.63	82.22	82.51	82.54
31.0	82.66	82.28	82.55	82.57

Appendix 1 (Continued)

Time (hrs.)	Stage in Colorado river (meter)	Potential at well #2 (meter)	Potential at well #3 (meter)	Potential at well #4 (meter)
31.5	82.67	82.33	82.58	82.60
32.0	82.68	82.36	82.60	82.61
32.5	82.69	82.39	82.62	82.63
33.0	82.71	82.42	82.63	82.64
33.5	82.71	82.43	82.63	82.64
34.0	82.72	82.45	82.64	82.65
34.5	82.73	82.46	82.65	82.65
35.0	82.74	82.47	82.66	82.67
35.5	82.74	82.48	82.66	82.68
36.0	82.64	82.45	82.60	82.60
36.5	82.55	82.39	82.52	82.51
37.0	82.40	82.29	82.38	82.37
37.5	82.22	82.18	82.22	82.20
38.0	82.01	82.06	82.04	82.01
38.5	81.78	81.93	81.85	81.80
39.0	81.54	81.81	81.70	81.60
39.5	81.33	81.70	81.56	81.41
40.0	81.13	81.61	81.45	81.30
40.5	80.95	81.53	81.38	81.20
41.0	80.81	81.45	81.29	81.11
41.5	80.68	81.39	81.22	81.04
42.0	80.58	81.33	81.16	81.00
42.5	80.50	81.27	81.11	80.94
43.0	80.44	81.22	81.06	80.90
43.5	80.39	81.17	81.01	80.86
44.0	80.35	81.13	80.97	80.82
44.5	80.33	81.09	80.93	80.79
45.0	80.31	81.06	80.90	80.77
45.5	80.29	81.02	80.87	80.75
46.0	80.29	80.99	80.84	80.71
46.5	80.28	80.97	80.82	80.70
47.0	80.28	80.94	80.80	80.69

Appendix 1 (Continued)

Time (hrs.)	Stage in Colorado river (meter)	Potential at well #2 (meter)	Potential at well #3 (meter)	Potential at well #4 (meter)
47.5	80.27	80.92	80.78	80.67
48.0	80.27	80.90	80.76	80.65
48.5	80.33	80.88	80.75	80.65
49.0	80.58	80.88	80.75	80.68
49.5	80.79	80.92	80.81	80.78
50.0	81.15	80.99	80.92	80.97
50.5	81.53	81.12	81.15	81.40
51.0	81.85	81.28	81.52	81.72
51.5	82.05	81.45	81.81	81.94
52.0	82.21	81.61	82.00	82.10
52.5	82.31	81.76	82.13	82.22
53.0	82.40	81.88	82.24	82.31
53.5	82.48	81.99	82.33	82.40
54.0	82.54	82.08	82.39	82.45
54.5	82.58	82.17	82.47	82.51
55.0	82.63	82.23	82.51	82.55
55.5	82.65	82.29	82.55	82.58
56.0	82.67	82.34	82.58	82.61
56.5	82.69	82.37	82.60	82.63
57.0	82.70	82.40	82.62	82.64
57.5	82.71	82.42	82.63	82.64
58.0	82.73	82.44	82.64	82.65
58.5	82.74	82.46	82.65	82.65
59.0	82.75	82.47	82.66	82.66
59.5	82.65	82.48	82.66	82.66
60.0	82.55	82.45	82.61	82.61
60.5	82.40	82.39	82.52	82.51
61.0	82.22	82.30	82.38	82.37
61.5	82.01	82.18	82.22	82.19
62.0	81.77	82.07	82.03	82.01
62.5	81.54	81.94	81.86	81.80
63.0	81.33	81.82	81.70	81.60

Appendix 1 (Continued)

Time (hrs.)	Stage in Colorado river (meter)	Potential at well #2 (meter)	Potential at well #3 (meter)	Potential at well #4 (meter)
63.5	81.13	81.71	81.56	81.43
64.0	80.95	81.62	81.45	81.30
64.5	80.81	81.53	81.38	81.19
65.0	80.68	81.46	81.30	81.11
65.5	80.58	81.39	81.23	81.05
66.0	80.50	81.33	81.17	81.00
66.5	80.43	81.28	81.11	80.94
67.0	80.39	81.23	81.06	80.90
67.5	80.35	81.18	81.02	80.86
68.0	80.32	81.14	80.98	80.82
68.5	80.31	81.10	80.94	80.80
69.0	80.30	81.06	80.91	80.77
69.5	80.29	81.03	80.88	80.75
70.0	80.28	81.00	80.85	80.73
70.5	80.28	80.97	80.83	80.70
71.0	80.27	80.95	80.80	80.68
71.5	80.27	80.92	80.78	80.67
72.0	80.32	80.90	80.76	80.65
72.5	80.48	80.88	80.75	80.65
73.0	80.76	80.88	80.75	80.68
73.5	81.15	80.92	80.80	80.77
74.0	81.56	80.99	80.92	80.96
74.5	81.87	81.13	81.16	81.41
75.0	82.10	81.29	81.56	81.75
75.5	82.27	81.48	81.87	82.00
76.0	82.40	81.66	82.07	82.17
76.5	82.50	81.83	82.23	82.31
77.0	82.56	81.98	82.34	82.42
77.5	82.60	82.08	82.42	82.48
78.0	82.63	82.17	82.48	82.53
78.5	82.65	82.24	82.52	82.56
79.0	82.67	82.30	82.56	82.60

Appendix 1 (Continued)

Time (hrs.)	Stage in Colorado river (meter)	Potential at well #2 (meter)	Potential at well #3 (meter)	Potential at well #4 (meter)
79.5	82.68	82.34	82.59	82.61
80.0	82.70	82.37	82.61	82.62
80.5	82.71	82.41	82.63	82.65
81.0	82.72	82.43	82.64	82.65
81.5	82.73	82.45	82.65	82.66
82.0	82.74	82.46	82.65	82.66
82.5	82.74	82.47	82.66	82.66
83.0	82.75	82.49	82.67	82.67
83.5	82.75	82.50	82.67	82.67
84.0	82.66	82.47	82.62	82.61
84.5	82.56	82.40	82.52	82.52
85.0	82.40	82.30	82.39	82.37
85.5	82.22	82.19	82.23	82.20
86.0	82.00	82.07	82.01	82.00
86.5	81.77	81.94	81.87	81.80
87.0	81.55	81.82	81.71	81.61
87.5	81.33	81.72	81.57	81.42
88.0	81.13	81.62	81.46	81.31
88.5	80.96	81.54	81.48	81.20
89.0	80.81	81.47	81.31	81.12
89.5	80.68	81.40	81.24	81.05
90.0	80.58	81.34	81.18	81.01
90.5	80.50	81.28	81.12	80.95
91.0	80.43	81.23	81.07	80.90
91.5	80.39	81.19	81.03	80.86
92.0	80.35	81.14	80.98	80.83
92.5	80.33	81.11	80.95	80.80
93.0	80.31	81.07	80.92	80.77
93.5	80.30	81.04	80.89	80.75
94.0	80.29	81.01	80.86	80.72
94.5	80.29	80.98	80.83	80.70
95.0	80.28	80.95	80.81	80.69

Appendix 1 (Continued)

Time (hrs.)	Stage in Colorado river (meter)	Potential at well #2 (meter)	Potential at well #3 (meter)	Potential at well #4 (meter)
95.5	80.28	80.93	80.79	80.67
96.0	80.27	80.91	80.77	80.66
96.5	80.27	80.89	80.75	80.65
97.0	80.49	80.89	80.76	80.68
97.5	80.77	80.92	80.81	80.78
98.0	81.14	81.01	80.93	80.96
98.5	81.53	81.13	81.15	81.39
99.0	81.85	81.30	81.54	81.73
99.5	82.09	81.48	81.84	81.98
100.0	82.27	81.66	82.06	82.17
100.5	82.40	81.84	82.22	82.31
101.0	82.48	81.98	82.33	82.39
101.5	82.55	82.09	82.41	82.46
102.0	82.60	82.17	82.48	82.52
102.5	82.65	82.25	82.54	82.57
103.0	82.67	82.31	82.57	82.59
103.5	82.69	82.35	82.59	82.61
104.0	82.71	82.38	82.61	82.63
104.5	82.72	82.41	82.64	82.63
105.0	82.73	82.44	82.65	82.64
105.5	82.73	82.46	82.65	82.65
106.0	82.74	82.47	82.66	82.66
106.5	82.74	82.49	82.67	82.67
107.0	82.75	82.50	82.68	82.68
107.5	82.75	82.51	82.68	82.68
108.0	82.66	82.48	82.62	82.62
108.5	82.56	82.41	82.53	82.53
109.0	82.41	82.31	82.39	82.38
109.5	82.22	82.20	82.21	82.21
110.0	82.01	82.08	82.06	82.02
110.5	81.78	81.96	81.88	81.81
111.0	81.55	81.83	81.71	81.61

Appendix 1 (Continued)

Time (hrs.)	Stage in Colorado river (meter)	Potential at well #2 (meter)	Potential at well #3 (meter)	Potential at well #4 (meter)
111.5	81.33	81.73	81.57	81.41
112.0	81.13	81.63	81.46	81.30
112.5	80.96	81.55	81.39	81.20
113.0	80.81	81.48	81.31	81.12
113.5	80.68	81.41	81.24	81.05
114.0	80.57	81.35	81.18	81.01
114.5	80.50	81.30	81.12	80.94
115.0	80.43	81.24	81.07	80.89
115.5	80.38	81.20	81.03	80.86
116.0	80.35	81.15	80.99	80.83
116.5	80.32	81.11	80.95	80.80
117.0	80.31	81.08	80.92	80.77
117.5	80.29	81.05	80.89	80.75
118.0	80.29	81.02	80.86	80.72
118.5	80.28	80.99	80.83	80.71
119.0	80.28	80.96	80.81	80.69
119.5	80.27	80.94	80.79	80.67
120.0	80.27	80.92	80.77	80.65

REFERENCES

1. Petersen, M., "River Engineering," Prentice-Hall, Inc. Englewood Cliffs, New Jersey, 1987.

2. Peck, R. B., Hanson, W. E. and Thornburn, T. H., "Foundation Engineering," 2nd edition, John Wiley & Sons, Inc., New York, 1974.

3. Desai, C. S., "Finite Element Residual Schemes for Unconfined Flow," International Journal of Numerical Methods in Engineering, 10, 1415, 1976.

4. Desai, C. S. and G. C. Li, "A Residual Flow Procedure and Application for Free Surface Flow in Porous Media," Advances in Water Resources, 6, 27, 1983.

5. Neuman, S. P. and Witherspoon, P. A., "Analysis of Nonsteady Flow with a Free Surface Using the Finite Element Method," Water Resources Research, Vol. 7, No. 3, 1971, pp. 611–623.

6. Neuman, S. P., "Saturated–Unsaturated Seepage by Finite Element Method," Journal of the Hydraulics Division, ASCE, Vol. 99, No. HY12, 1973, pp. 2233–2251.

7. Liggett, J. A., "Location of Free Surface in Porous Media," Journal of the Hydraulics Division, ASCE, Vol. 103, No. HY4, 1977, pp. 353–365.

8. Liggett, James A. and Liu, Philip L-F, "The Boundary Integral Equation Method for Porous Media Flow," George Allen & Unwin (Publishers) Ltd.,1983.

9. Brebbia, C. A., Telles, J. C. F. and Wrobel, L. C., "Boundary Element Techniques," Springer-Verlag (publishers), 1984.